Thesis for the Degree

of Master

The Effects of Pileup Events with 7 TeV Proton-Proton Collision Data in the LHC

by

Seong-Gu Heo

Department of physics

Graduate school

Kangwon National University

February, 2011

Under the Guidance of

Professor Soon-Kown Nam

The Effects of Pileup Events with 7 TeV Proton-Proton Collision Data in the LHC

A THESIS

Submitted to the Graduate School of

Kangwon National University in Partial

Fulfillment of the Requirements

For the Degree of

Master of Science

by

Seong-Gu Heo

Department of Physics

February, 2011

Approved by Committee of the Graduate School of
Kangwon National University in Partial Fulfillment of
The Requirements for the Degree of
Master of Science

Seong-Gu Heo

December, 2010

Thesis Committee;

Soon-Kwon Nam (signature)

(Chairman of Committee)

Kang Il Lee (signature)

(Committeeman)

Ki-Bum Kim (signature)

(Committeeman)

The Effects of Pileup Events with 7 TeV Proton-Proton Collision Data in the LHC

Seong-Gu Heo

Department of physics

Graduate school, Kangwon National University

Abstract

The event analysis codes were developed to compare the magnitudes of track multiplicity, jet multiplicity, HT, MHT, MPT and |ΔØ | for the case of pileup and non-pileup events. And their correspondences between the Monte Carol simulation and the LHC 7 TeV proton-proton collision data were investigated. The event analysis codes executed HT, MHT, MPT and |ΔØ | calculations with jet, photon, CaloJets and vertex processes. All the data analysis was performed with CMSSW_3_8_4, SusyPAT, Root and CRAB. The event analysis and histogram codes were implemented by C and Python language respectively. The effects of pileup events were well shown in the track multiplicity. The correspondences between MC and collision data showed a good agreement with jet p_T cut 30 GeV. The |ΔØ| distributions of QCD_ p_T 30 GeV and collision data with jet p_T cut 30 GeV were well agreed showing expected enhancements near 0 and π.

CONTENTS

List of Figures

I. Introduction

1. Cern large hardron collider and compact muon solenoid detector

The CERN Large Hadron Collider (LHC) is a new tool to test the Standard Model. The LHC is built in a circular tunnel 27 km in circumference and about 50 to 175 m underground. The overall layout of the LHC machine is shown in Figure 1. Two proton beams are injected into each of the twin LHC synchrotron and accelerated. The two beams are focused and brought into collision at the four interaction points. The LHC aims at producing 14 TeV proton-proton collisions but has been producing 7 TeV collisions yet. There are 100 billion protons per bunch at the interaction point. The Compact Muon Solenoid detector (CMS) is one of the four major detectors of the LHC [1]. The overall dimensions of the CMS detector are a length of 21.6 m, a diameter of 14.6 m and a total weight of 12,500 tons. Its sub-detectors are Silicon Tracker, Electromagnetic Calorimeter (Ecal), Hadron Calorimeter (Hcal) and Muon Systems from Its center, which are shown in Figure 2.

2. CMS event data model (EDM)

The event data holds all data that were taken during a physics event. Events are processed by passing a sequence of modules. The event class represents the observed and inferred products of a single triggered readout of the CMS detector. The event is responsible for managing the lifetime of and relationships between the contents of the data. The contents of the event can include objects representing the raw detector output, reconstruction products, simulation products, and analysis objects relating to a single beam crossing or simulation. CMS uses a number of event data formats. Raw data (RAW) contain the detector data, the level one (L1) trigger result, the result of the high level trigger (HLT) selections, and some of the higher-level objects created during HLT processing. Reconstructed data (RECO) are the data created by the event reconstruction program. They are derived from RAW data and provides access to reconstructed physics objects for physics analysis. Analysis object data (AOD) derived from the RECO data to provide data for physics analysis in a convenient and compact format. The AOD contain enough information about the event to support all the typical usage patterns of a physics analysis [2]. The CMS event model is shown in Figure 3. Due to the high luminosity, the LHC produces pileup events in single bunch crossing. The addition of pileup collisions occurs much faster than the detector simulation and it depends on the LHC luminosity and run conditions. Therefore, pileup collisions are simulated separately from the signal collisions and they are merged in a second step using a luminosity dependent pileup contribution [3]. The pileup simulation is performed using GEANT4 toolkit [4].

3. CMS computing systems

The CMS computing environment is a distributed system of computing services and resources. The set of services and their behavior together provide the CMS computing system as part of the Worldwide LHC Computing Grid (WLCG). Some of the services implementing particular CMS application behavior are virtual organization (VO) specific. Figure 4 shows the overall architecture of the CMS computing system. Grid Workload Management System (WMS) allows CMS to make use of and access distributed computing resources. The overview of the CMS workflow management system is shown in Figure 4. The Computing Elements (CE) declare themselves available and publish information about their status and resources. The baseline solution for a Grid WMS is shown in Figure 5. CMS users can submit jobs to the WMS via gLite and with CMS e-certificate. The jobs are sent to WMS with the requirements that the

CE has access to the Storage Element (SE) where the data are located. The WMS is the connection between the user, who works on the User Interface (UI) and the CE. The CMS Data Management (DM) system provides the basic infrastructure and tools allowing CMS users to discover, access and transfer event data in a distributed computing environment. Other CMS specific services support specific needs of CMS applications and software [2].

4. Definitions

The Pixel detector provides high resolution and three-dimensional space points. Using the pixel data, tracks and primary vertices can be found [5]. The prompt tracks originating from the primary interaction region are selected based on the transverse impact parameter significance with respect to the beam line. The selected tracks are then clustered based on their z coordinates at the point of closest approach to the beam line. Vertex candidates are formed by grouping tracks that are separated in z by less than 1 cm from their nearest neighbor. Candidates containing at least two tracks are then fit with an adaptive vertex fit to compute the best estimate of vertex parameters such as position [6]. Tracks are reconstructed from the signal information deposited on the Trackers. Jets are reconstructed from the information deposited on Hadron Calorimeter. These jets are called as CaloJets and they are used to calculate the transverse momentum scalar sum (HT) in this thesis. The large missing transverse momentum plus jets final state topology has a great potential for discovery of new physics involving dark matter candidates. MHT is the missing transverse momentum vector sum which is calculated from the Hadron Calorimeter deposited energy. MPT is the missing transverse momentum vector sum which is calculated from the tracker deposited energy. $|\Delta Ø|$ is the angle between MHT and MPT. The large missing transverse momentum plus jets final state topology has great potential for discovery of new physics including dark matter candidates. Some Standard Model processes can produce the same jets plus missing energy signature. One of the main Standard Model backgrounds is expected to be from QCD multi-jets production. MPT azimuthal angle can be compared to the one of the calorimetry-based missing transverse momentum, giving rise to a new handle to clean away QCD events with large miss-measurements. This angular difference can be used to maintain high signal efficiency on event s with real missing energy (MET), while providing additional QCD rejection [5, 6]. The characteristics of MPT have been used at the Tevatron and D0 searches as an additional handle to separate miss-measurements from real MET [7, 8].

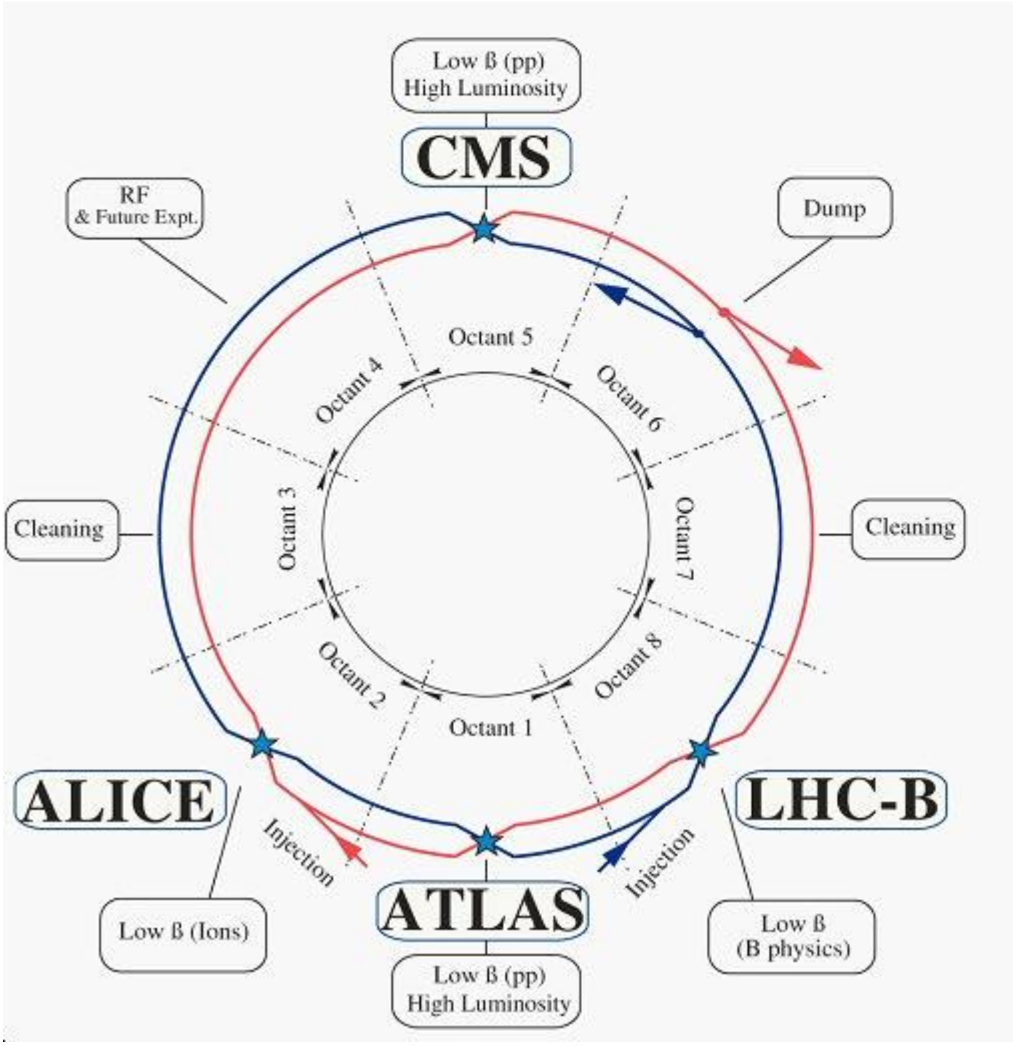

Fig. 1. Overall layout of the LHC machine

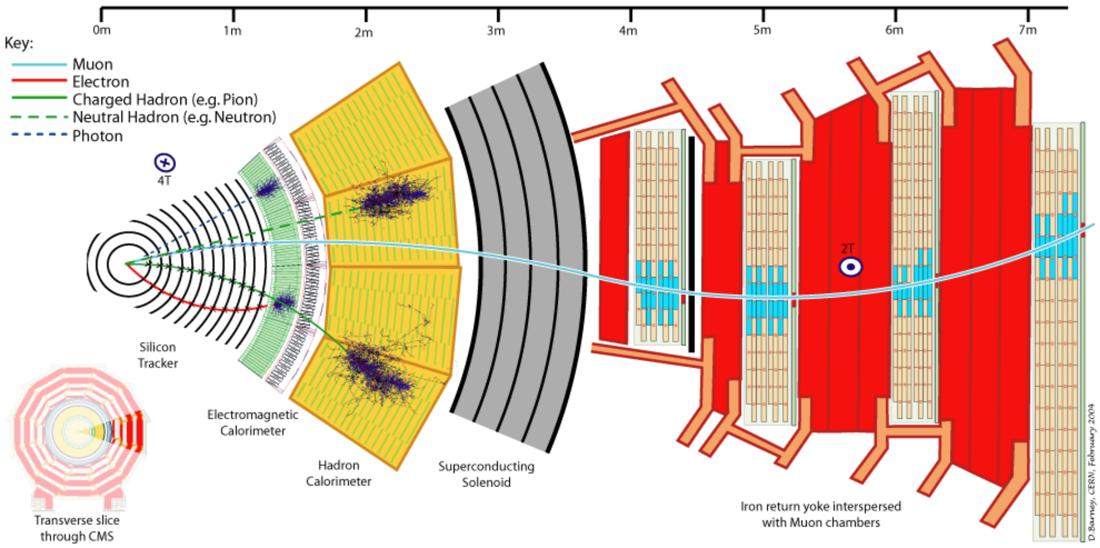

Fig. 2. Compact muon solenoid detector.

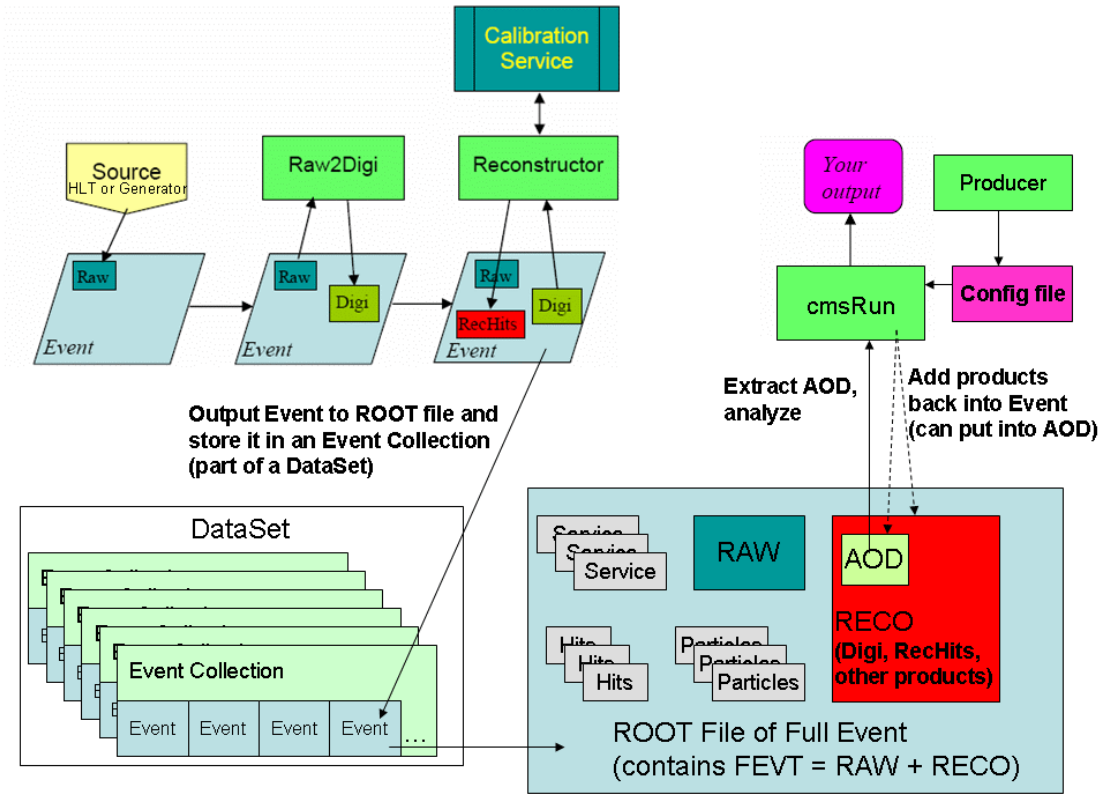

Fig. 3. CMS event data model.

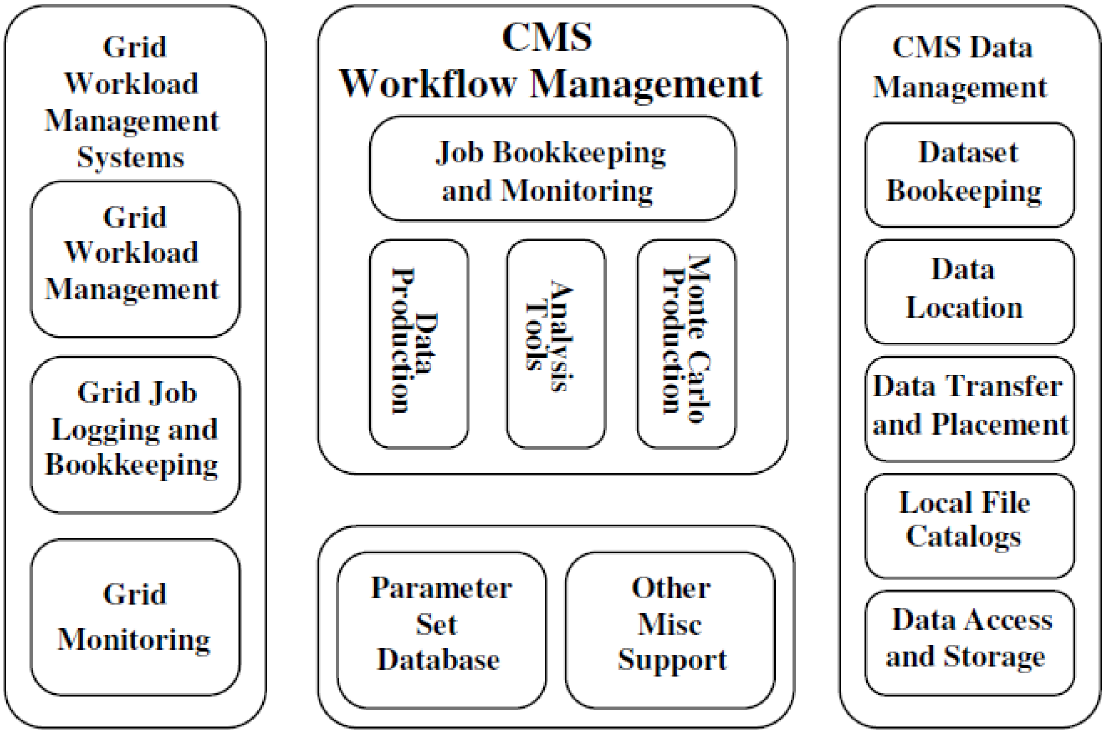

Fig. 4. Overview of systems and services supporting the CMS workflow management system.

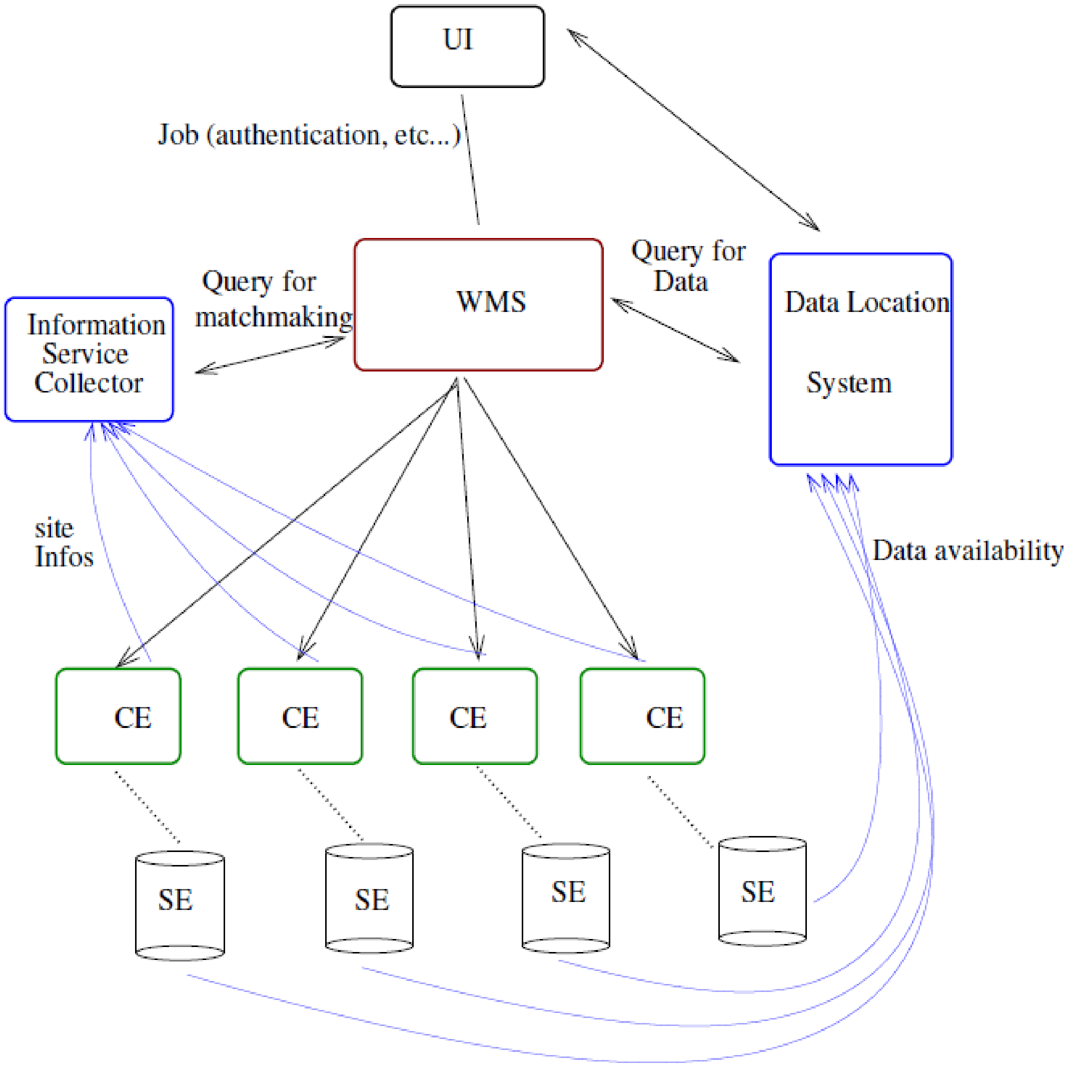

Fig. 5. Schematics showing the baseline WMS architecture.

II. The effects of pileup events

1. Data sets and software

MC data sets, "/QCD_ Pt 15/Summer10-START3X_V26_S09-v1/GEN-SIM-RECODEBUG" (QCD_ p_T 15 GeV) and "/QCD_ Pt 30/Summer10-START3X_V26_S09-v1/GEN-SIM-RECODEBUG" (QCD_ p_T 30 GeV) and collision data set,
"/JetMETTau/Run2010A-PromptReco-v4/RECO" are used for the analysis. Luminosity block ranges are analyzed according to the "Cert_132440-144114_7TeV_StreamExpress_Collisions10_JSON_v2" data certification for the collision data. The analysis starts from run number 138564, which was collected after the month-long LHC commissioning period in June and expected to have more pileup events than in the data period before. The total number of events is about 1 million for the collision data set and 5 millions for each MC data set. All data sets are analyzed by the event analysis codes we developed and the standard SusyPAT recipe [7].

2. Event analysis code implementation

The sequential recombination algorithms examine four-vector inputs pair wise and construct jets. They construct the quantities

$$d_{ij} = \min\left(p_{Ti}^{n}, p_{Tj}^{n}\right) \Delta D_{ij}^{2}/D^{2} \tag{1}$$

where p_{Ti} is the transverse momentum of the i-th particle with respect to the beam axis, ΔD_{ij} is the distance between particles i and j and D is the radius parameter. The case of n

= -2 corresponds to the ”anti-k_T” algorithm [8-9]. CaloJets are reconstructed with the anti-k_T algorithm with D = 0.5. The SusyPAT creates PAT(Physics Analysis Tool) objects from the “standard” RECO(Reconstruction Objects) objects provided by the CMS reconstruction and stores many observables used in SUSY searches in the output file. With command line options, “SUSY_pattuple_cfg.py generates “SusyPAT_cfg.py”. For the collision data, all events are required to pass the high level trigger (HLT_Jet30U), which requires at least one jet with an uncorrected transverse momentum of at least 30 GeV at the HLT level. The “SusyPAT_cfg.py” is submitted to the grid computing pool via CRAB [10]. CRAB brings the output files containing PAT objects.

The output files are processed via the event analysis code which executes HT , MHT, MPT and |ΔØ | calculations with jet, photon, CaloJets and vertex processes. Jet processes require energy fraction greater than 0.01. Photons are taken from the standard photon collection with photon identification flag “PhotonCutBasedIDLoose”. Photon fake p_T cut is 10 GeV. For this study, tracks are taken from the general tracks collection without p_T cut, but filtered with high purity requirement. QCD events are characterized by a large multiplicity of low p_T tracks. The high purity quality flag provides a high efficiency and low fake rate for such tracks. PyROOT process the output files which come after running the C code and gets the analysis histograms [11].

3. Tracks, jets and HT analysis

One primary vertex event has five jets and many tracks as shown in Figure 6 (a). Two primary vertices event has two primary vertices and some tracks but no jets as shown in Figure 6 (b). The event of three primary vertices is shown in Figure 6 (c). It has three primary vertices and some tracks and only one jet. One primary vertex events are called as non-pileup events. On the other hand, more than one primary vertex events are called as pileup events. Pileup events are expected to have more tracks and jets than non-pileup events.

The distributions of the track multiplicities of the collision data at vertex = 1, 2, 3 and ≥ 4 are shown in Figure 7. The multiplicities increase as the number of vertex becomes bigger showing a clear pileup effect. The correspondences of the track multiplicity between the MC and collision data normalizing to the simulation data are shown in Figure 8 and 9. Figure 8 (a) - (c) show the correspondence between QCD_ p_T 15 GeV and collision data with jet p_T cut 15 GeV at vertex = 1, 2 and 3. Figure 9 (a) - (c) show the correspondence between QCD_ p_T 30 GeV and collision data with jet p_T cut 30 GeV. The correspondences show a good agreement with the tracks whose multiplicity is less than about 100 for both pileup and non-pileup events.

Jets are experimental signatures of quarks and gluons, which are produced in high energy processes such as the hard scattering of partons in proton-proton collisions. Calorimeter jets are reconstructed using energy deposits in the electromagnetic (ECAL) and hadronic (HCAL) calorimeter cells, combined into calorimeter towers. A calorimeter tower consists of one or more HCAL cells and the geometrically corresponding ECAL crystals [12]. Combined with the fact that typical SUSY-like events have a large jet multiplicity, a large number of tracks is expected in multijet events [13]. Figure 10 (a) – (c) shows the jet multiplicities of the collision data at jet p_T cut 10, 15 and 30 GeV with the number of vertex = 1, 2, 3 and ≥ 4. The effect of pileup events is shown clearly where jet p_T cut is 10 GeV. But the effect is weakened where the p_T cut is 15 and 30 GeV. This shows that the low p_T jets are dominant in the pileup effects. Overall, the effect of the pileup events becomes apparent as showing the multiplicities become bigger. The correspondences of the jet multiplicity between the

MC and collision data normalizing to the simulation data are shown in Figure 11 and 12. Figure 11 (a) – (c) show the correspondence between QCD_ p_T 15 GeV and collision data with jet p_T cut 15 GeV at vertex = 1, 2 and 3. Figure 12 (a) - (c) show the correspondence between QCD_ p_T 30 GeV and collision data jet p_T cut 30 GeV at vertex = 1, 2 and 3. For the case of jet p_T cut 15 GeV, the collision data agrees with the MC data with the relative error of about 18%. But for the case of jet p_T cut 30 GeV, the collision data shows a good agreement with the MC data with the relative error of about 8%.

The HT is the transverse momentum scalar sum which is calculated based on the jets.

$$\mathrm{HT} = \sum_i |p_T(\mathrm{jet}_i)| \tag{2}$$

The HT distributions of the collision data at vertex = 1, 2, 3 and ≥ 4 are shown in Figure 13. As the number of vertex increases, the mean of the HT becomes also increases. This shows a clear pileup effects on the HT. The correspondences of the HT between the MC and collision data normalizing to the simulation data are shown in Figure 14 and 15. Figure 14 (a) – (c) show the correspondence between QCD_ p_T 15 GeV and collision data with jet p_T cut 15 GeV at vertex = 1, 2 and 3. Figure 15 (a) – (c) show the correspondence between QCD_ p_T 30 GeV and collision data jet p_T cut 30 GeV at vertex = 1, 2 and 3. The correspondence distributions show a good agreement with jet p_T cut is 30 GeV

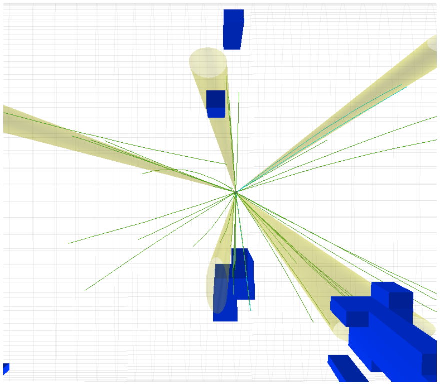

(a)

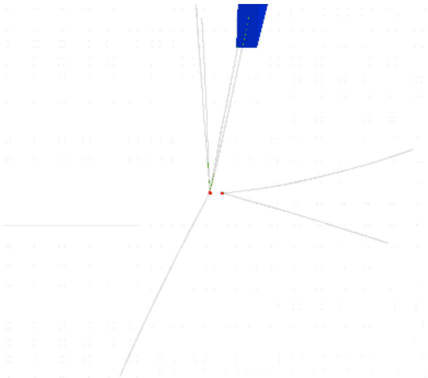

(b)

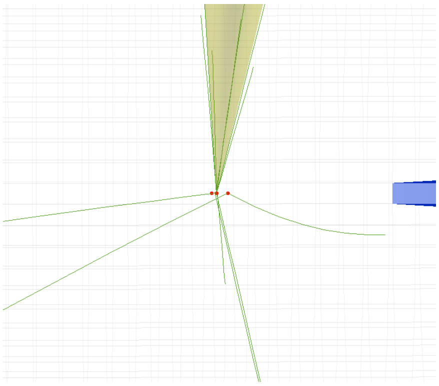

(c)

Fig. 6. One primary vertex (a), two primary vertices (b) and three primary vertices event (c).

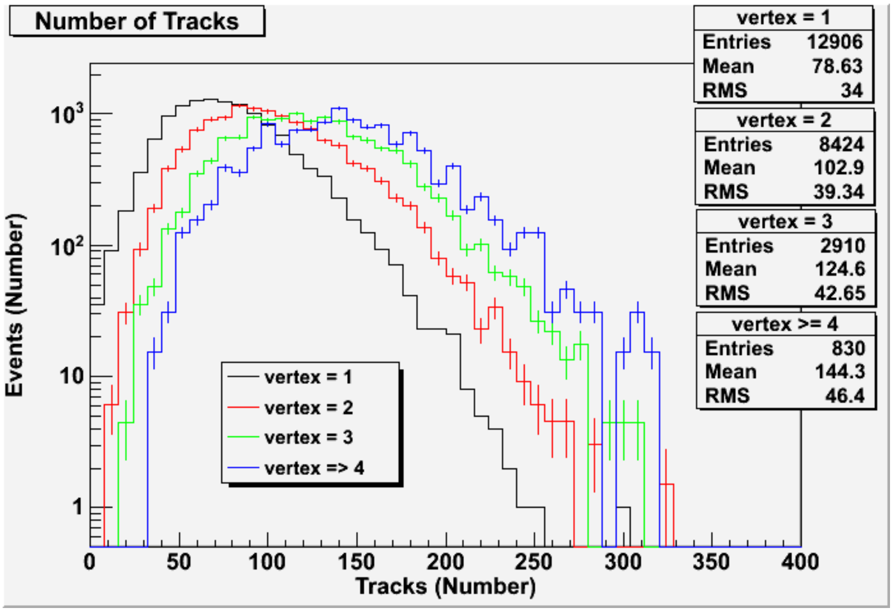

Fig. 7. Track multiplicity distributions at vertex = 1, 2, 3 and ≥ 4.

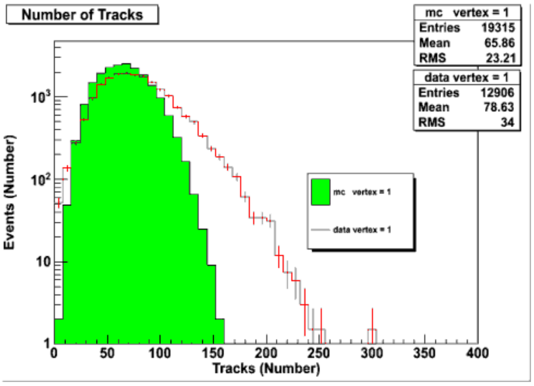

(a)

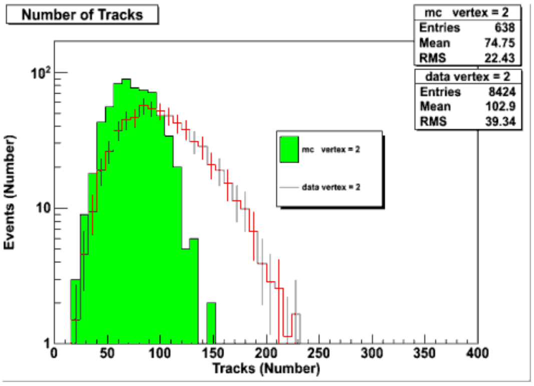

(b)

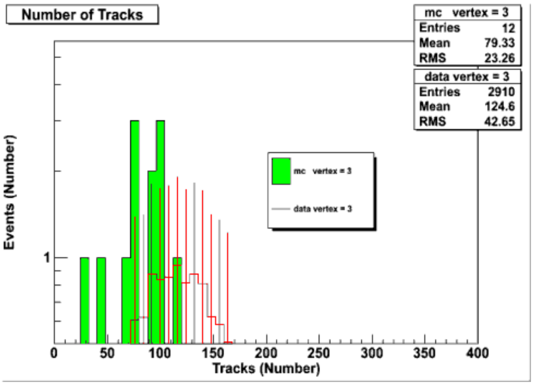

(c)

Fig. 8. Comparisons of track multiplicity distributions between QCD_ p_T 15 and collision data with jet p_T cut 15 GeV at vertex = 1 (a), 2 (b) and 3 (c).

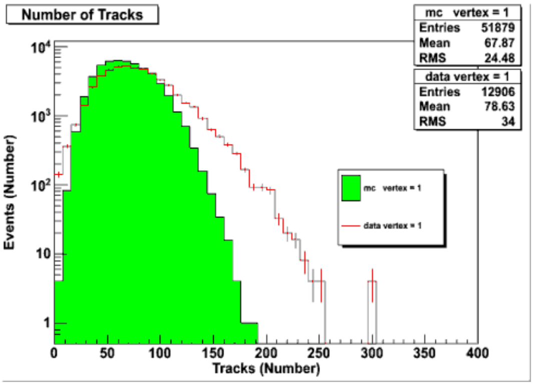

(a)

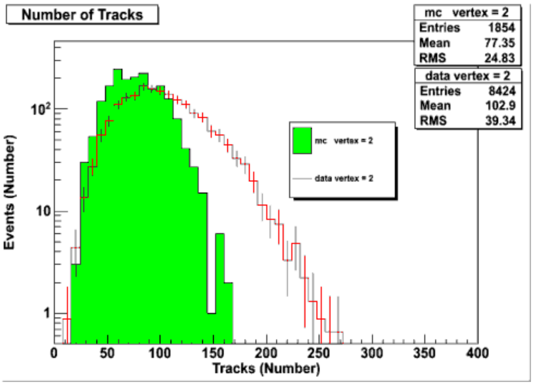

(b)

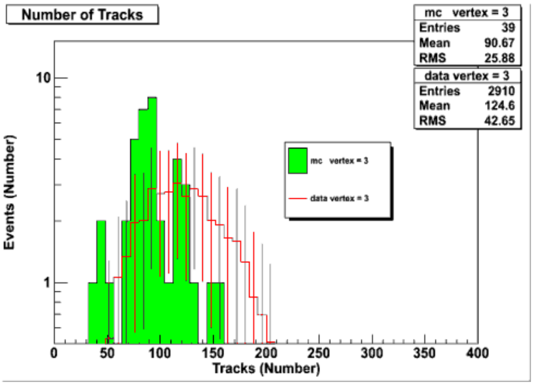

(c)

Fig. 9. Comparisons of track multiplicity distributions between QCD_ p_T 30 and collision data with jet p_T cut 30 GeV at vertex = 1 (a), 2 (b) and 3 (c).

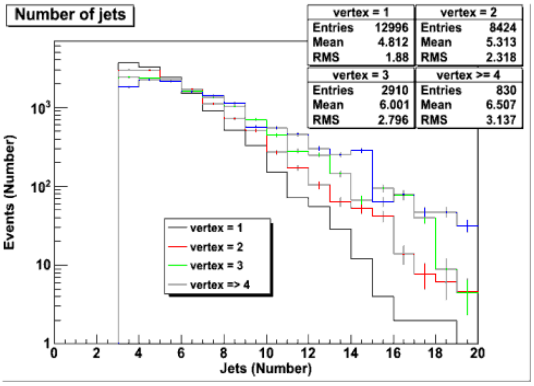

(a)

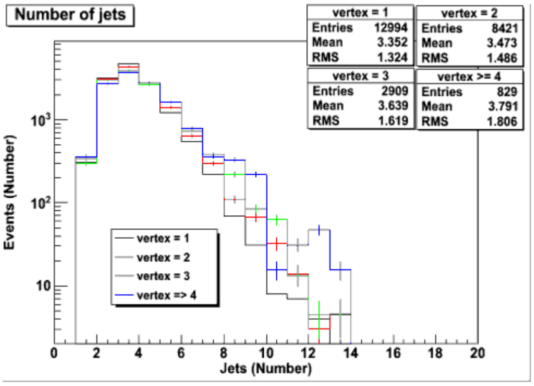

(b)

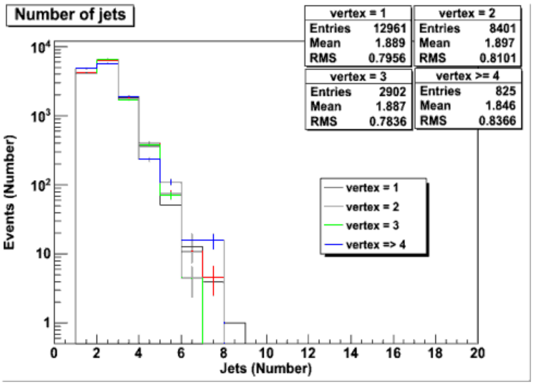

(c)

Fig. 10. Jet multiplicity distributions at vertex = 1, 2, 3 and ≥ 4 for jet p_T cut 10 (a), 15 (b) and 30 GeV (c).

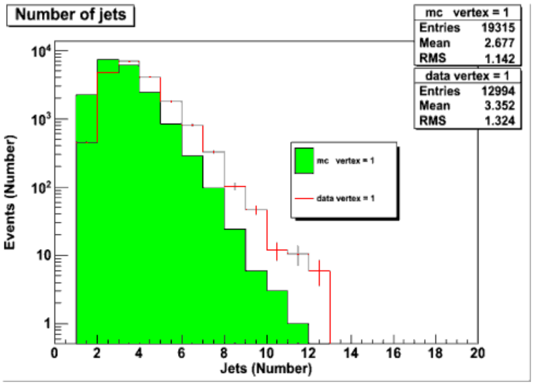

(a)

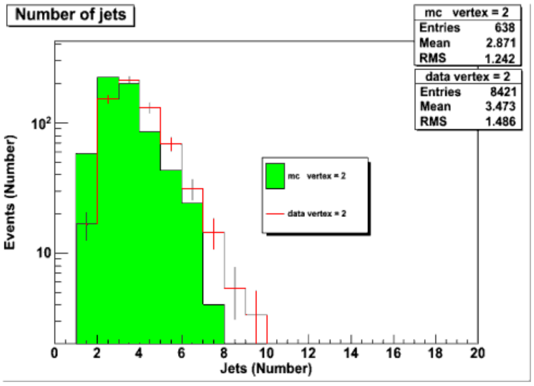

(b)

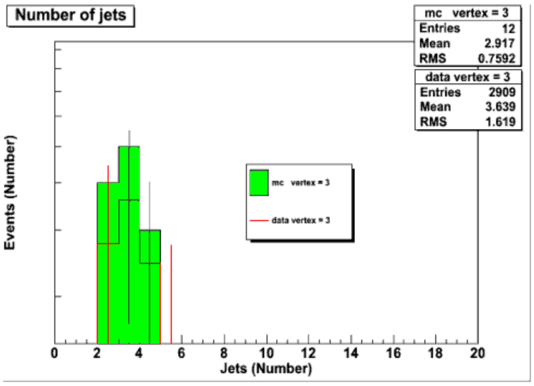

(c)

Fig. 11. Comparisons of jet multiplicity distributions between QCD_ p_T 15 and collision data with jet p_T cut 15 GeV at vertex = 1 (a), 2 (b) and 3 (c).

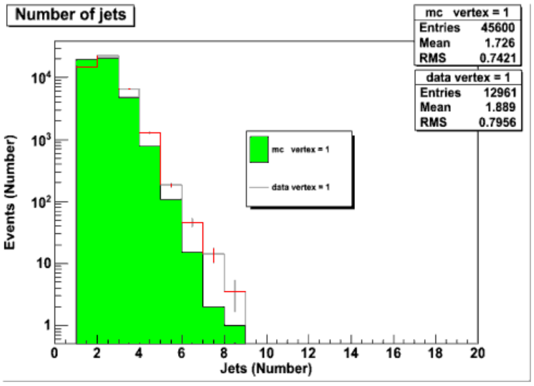

(a)

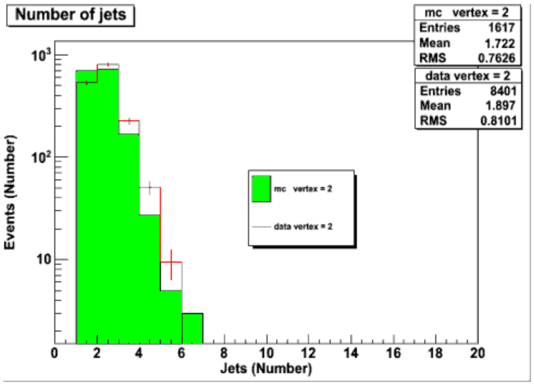

(b)

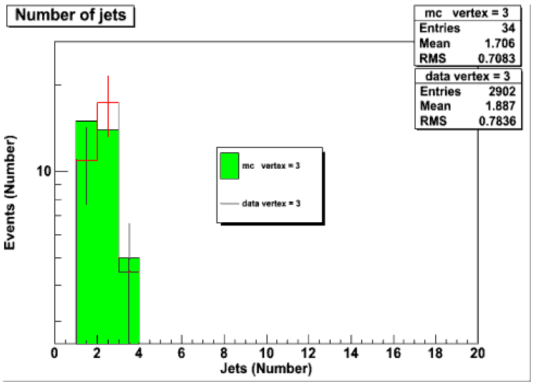

(c)

Fig. 12. Comparisons of jet multiplicity distributions between QCD_ p_T 30 and collision data with jet p_T cut 30 GeV at vertex = 1 (a), 2 (b) and 3 (c).

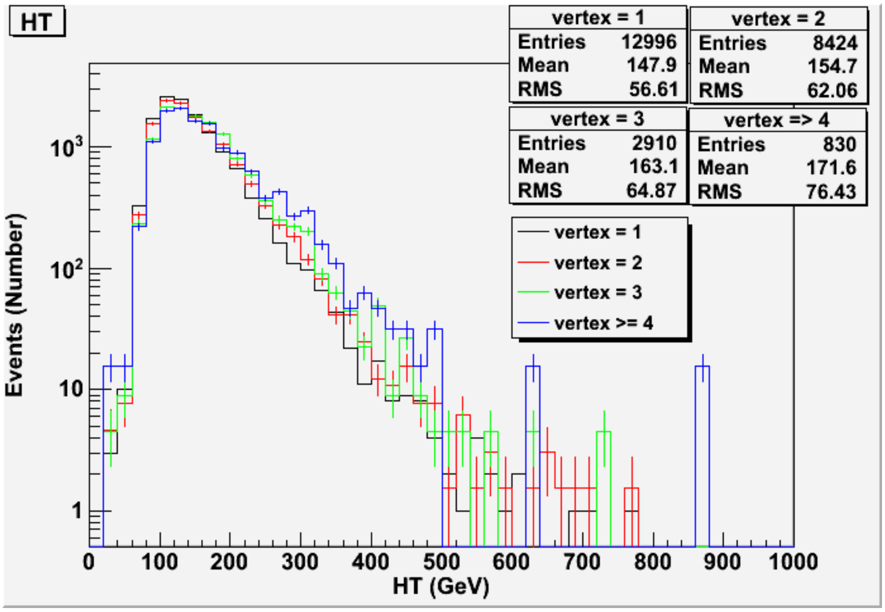

Fig. 13. HT distributions of 7 TeV collision data at vertex = 1, 2, 3 and ≥ 4.

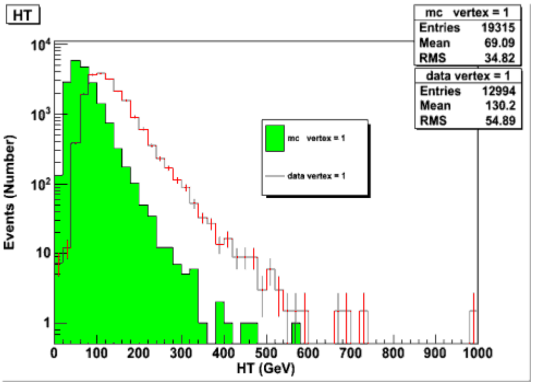

(a)

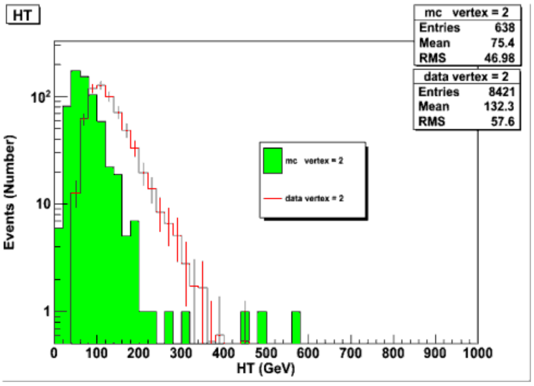

(b)

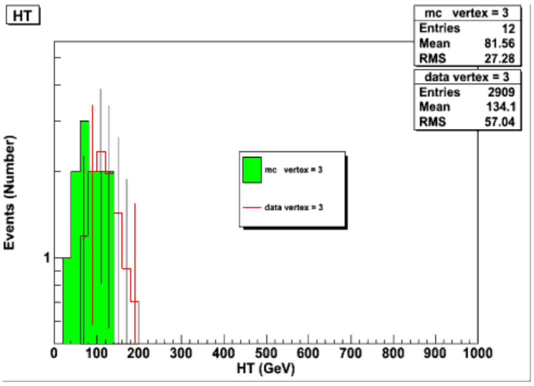

(c)

Fig. 14. Comparisons of HT distributions between QCD_ p_T 15 and collision data with jet p_T cut 15 GeV at vertex = 1 (a), 2 (b) and 3 (c).

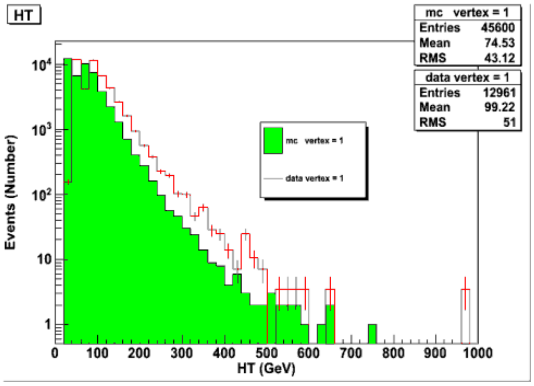

(a)

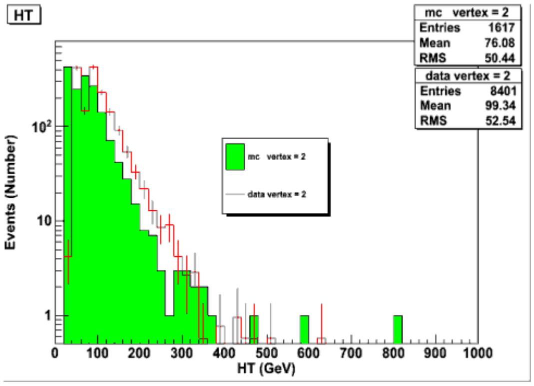

(b)

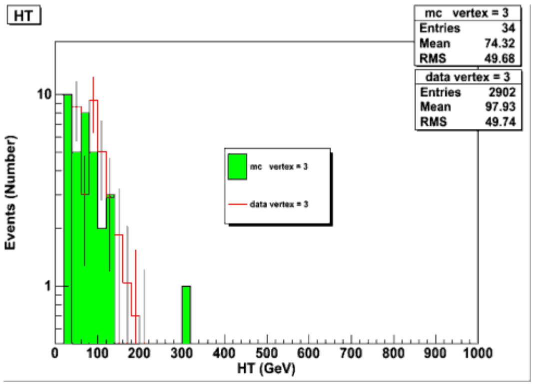

(c)

Fig. 15. Comparisons of HT distributions between QCD_ p_T 30 and collision data with jet p_T cut 30 GeV at vertex = 1 (a), 2 (b) and 3 (c).

4. MHT, MPT and $|\Delta\emptyset|$ Analysis

Missing transverse momentum (MHT) is defined as a negative vector sum of the transverse momentum of all hard physics objects, like jets, electrons, muons etc [14]. In this study the MHT is the missing transverse momentum vector sum of CaloJets.

$$\mathrm{MHT} = |-\textstyle\sum_i p_T(\mathrm{jet}_i)| \tag{3}$$

The MHT distributions of the collision data at vertex = 1, 2, 3 and $\geq$ 4 are shown in Figure 16. The distributions show the effect of the pileup events with jet p_T cut 10 and 15 GeV with the increment of the MHT mean value. The correspondences of the MHT between the MC and collision data normalizing to the simulation data are shown in Figure 17 and 18. Figure 17 (a) – (c) show the correspondence between QCD_ p_T 15 GeV and collision data with jet p_T cut 15 GeV at vertex = 1, 2 and 3. Figure 18 (a) – (c) show the correspondence between QCD_ p_T 30 GeV and collision data with jet p_T cut 30 GeV. The distributions show a good agreement in the events of vertex number one and two. But for the case of vertex = 3, there is no enough statistics to tell the correspondences.

MPT is the missing transverse momentum vector sum of the tracks in the events.

$$\mathrm{MPT} = |-\textstyle\sum_i p_T(\mathrm{track}_i)| \tag{4}$$

The distributions of the MPT of the collision data at vertex = 1, 2, 3 and $\geq$ 4 are shown in Figure 19. The MPT decreases as the number of vertex increases. The correspondences of the MPT between the MC and collision data normalizing to the simulation data are shown in Figure 20 and 21. Figure 20 (a) – (c) show the correspondence between QCD_ p_T 15 GeV and collision data with jet p_T cut 15 GeV at vertex = 1, 2 and 3. Figure 21 (a) – (c) show the correspondence between QCD_ p_T 30 GeV and collision data jet p_T cut 30 GeV at vertex = 1, 2 and 3. For the case of jet p_T cut 15 GeV, the relative error of the MPT mean value between the MC and collision data is about 33%. But for the case of jet p_T cut 30 GeV, the relative error of the MPT mean value between the MC and collision data is about 13%. This shows a better agreement with jet p_T cut 30 GeV than 15 GeV.

In QCD events where one of the jets has a large energy miss-measurement, the MHT will either be aligned or point in the opposite direction of that jet. The direction of MPT also follows the preferred transverse axis. Therefore it is expected to find for QCD events an enhancement near 0 and π in the distribution of the |ΔØ| [2]. The |ΔØ| distributions of the collision data at vertex = 1, 2, 3 and ≥ 4 are shown in Figure 22. The |ΔØ| distributions are more inclined to near 0 and π as the jet p_T cut increases. This tendency is shown the same in both pileup and non-pileup events. The correspondence of the MPT between the MC and collision data normalizing to the simulation data are shown in Figure 23 and 24. Figure 23 (a) – (c) show the correspondence between QCD_ p_T 15 GeV and collision data with jet p_T cut 15 GeV at vertex = 1, 2 and 3. Figure 24 (a) – (c) show the correspondence between QCD_ p_T 30 GeV and collision data jet p_T cut 30 GeV at vertex = 1, 2 and 3. QCD_ p_T 15 GeV data are inclined to π and the collision data with jet p_T cut 15 GeV also show the same inclination. QCD_ p_T 30 GeV MC data are evenly inclined to 0 and π. And the expected enhancements are shown in the collision data with jet p_T cut 30 GeV. Overall, The |ΔØ| distributions of QCD_ p_T 30 GeV and collision data with jet p_T cut 30 GeV show good agreements at vertex = 1 and 2. For the case of vertices 3, there is no enough statistics to examine the correspondence.

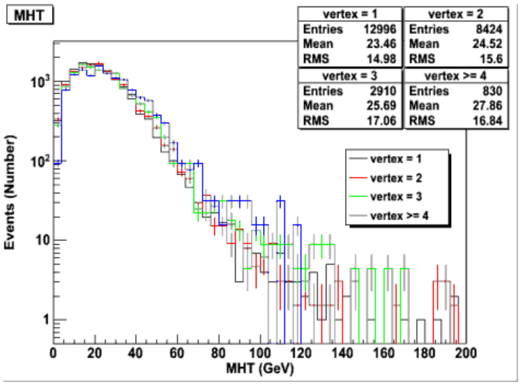

(a)

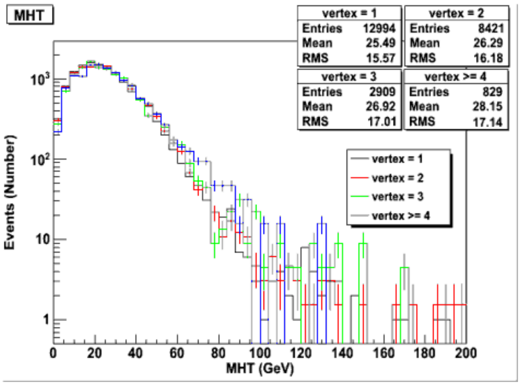

(b)

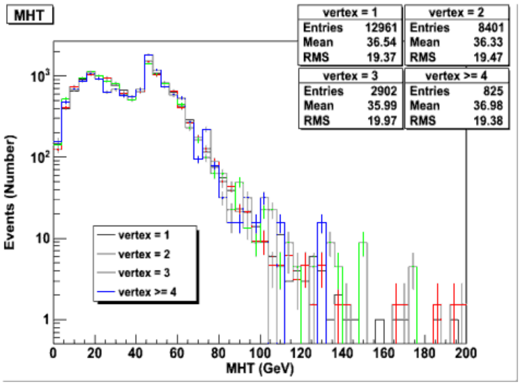

(c)

Fig. 16. MHT distributions at vertex = 1, 2, 3 and $\geq$ 4 for jet p_T cut 10 (a), 15 (b) and 30 GeV (c).

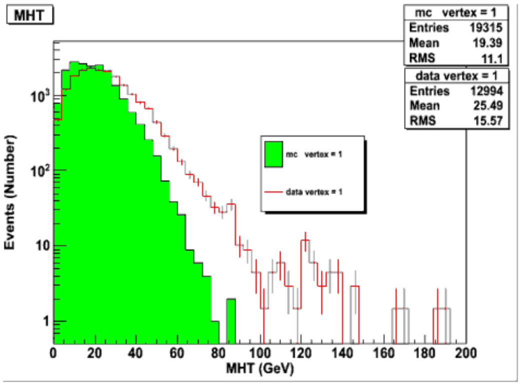

(a)

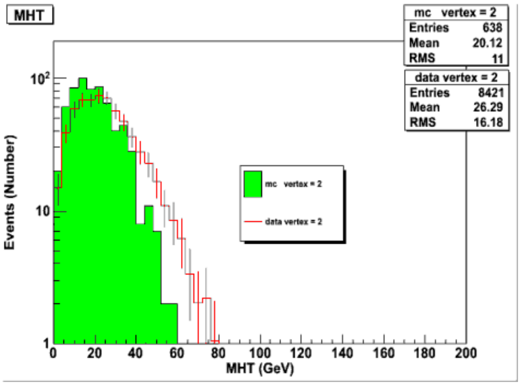

(b)

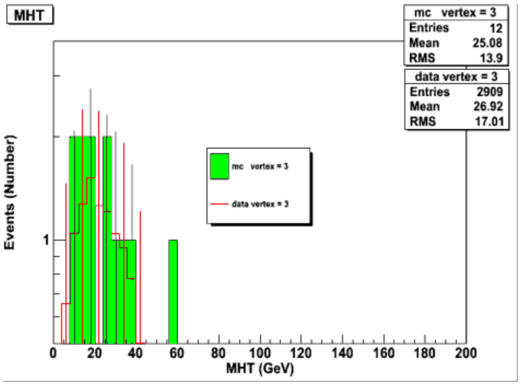

(c)

Fig. 17. Comparisons of MHT distributions between QCD_ p_T 15 and collision data with jet p_T cut 15 GeV at vertex = 1 (a), 2 (b) and 3 (c).

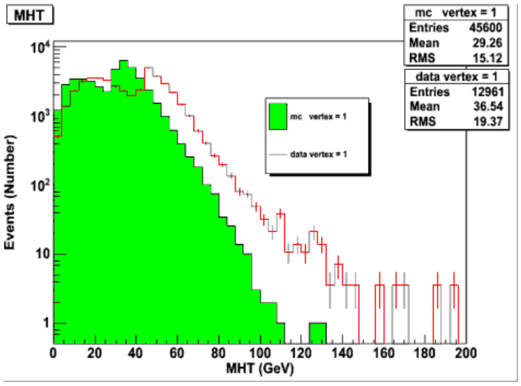

(a)

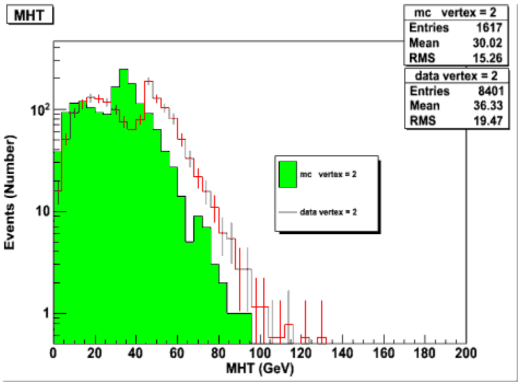

(b)

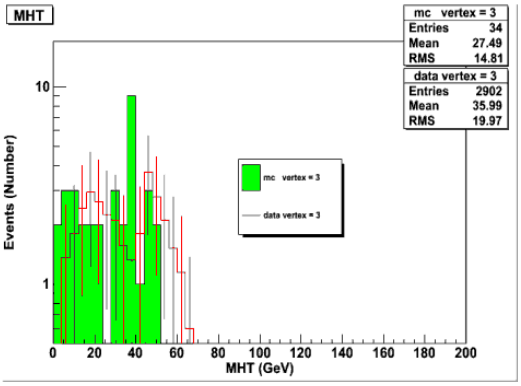

(c)

Fig. 18. Comparisons of MHT distributions between QCD_ p_T 30 and collision data with jet p_T cut 30 GeV at vertex = 1 (a), 2 (b) and 3 (c).

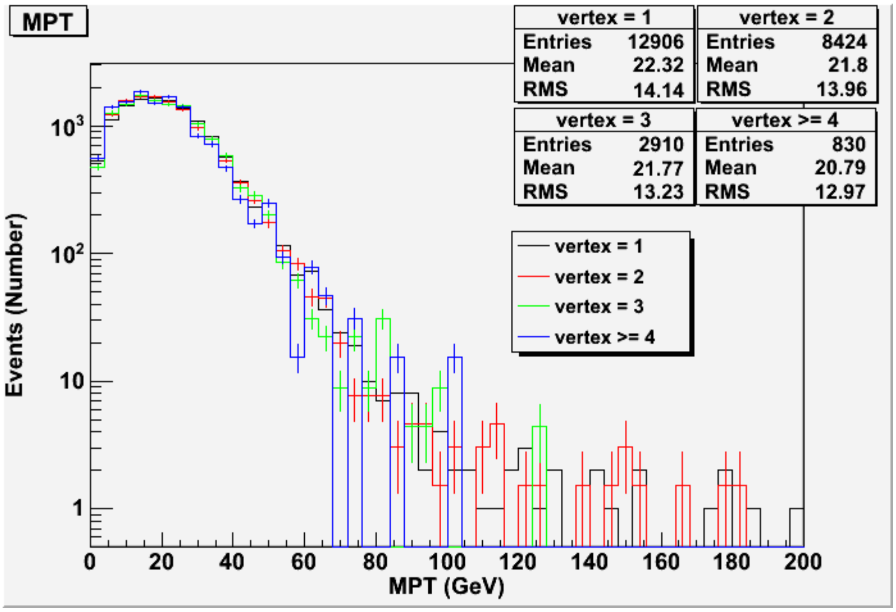

Fig. 19. MPT distributions of 7 TeV collision data at vertex = 1, 2, 3 and ≥ 4.

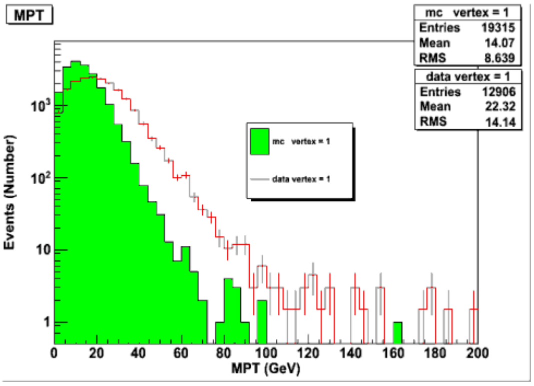

(a)

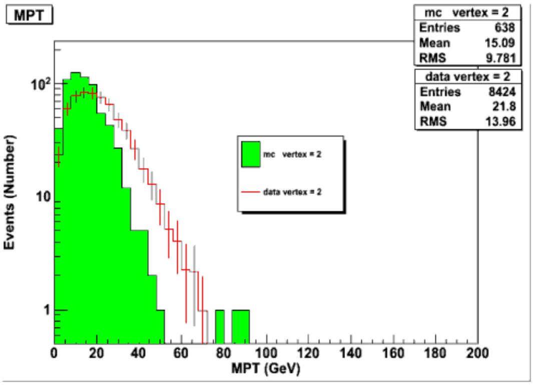

(b)

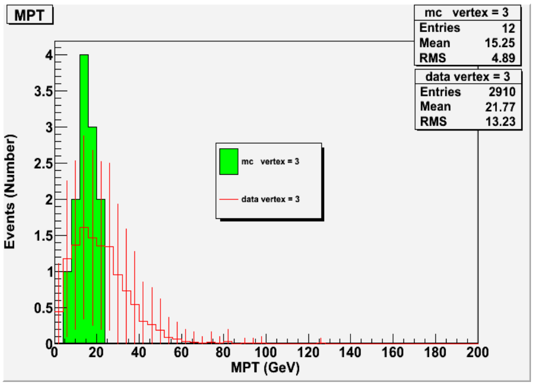

(c)

Fig. 20. Comparisons of MPT distributions between QCD_ p_T 15 and collision data with jet p_T cut 15 GeV at vertex = 1 (a), 2 (b) and 3 (c).

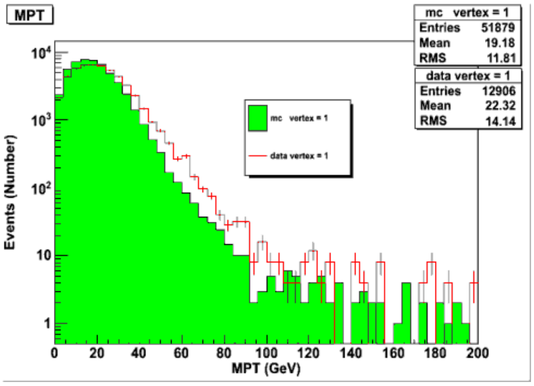

(a)

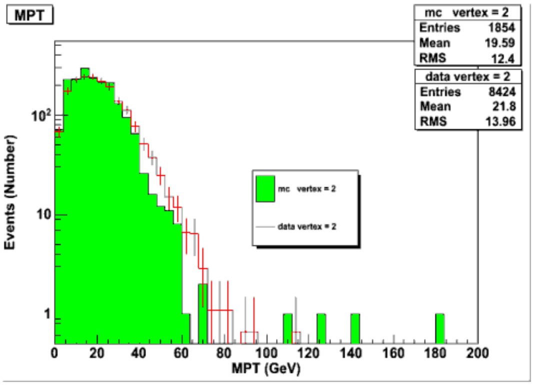

(b

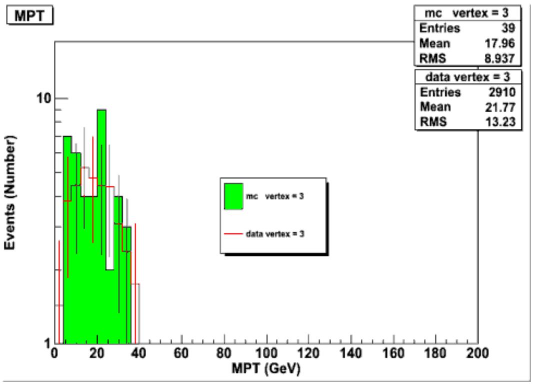

(c)

Fig. 21. Comparisons of MPT distributions between QCD_ p_T 30 and collision data with jet p_T cut 30 GeV at vertex = 1 (a), 2 (b) and 3 (c).

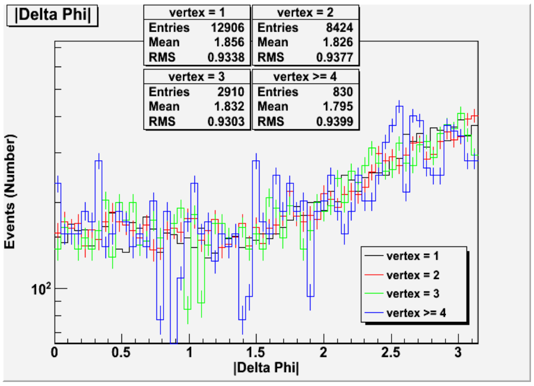

(a)

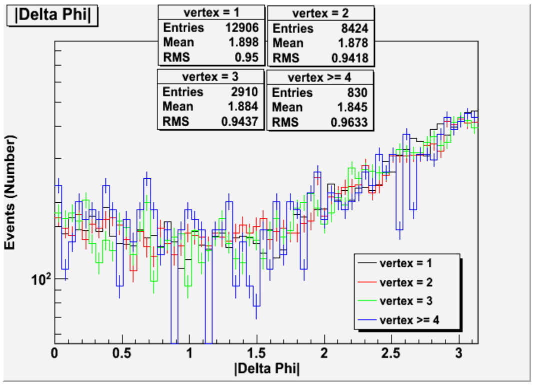

(b)

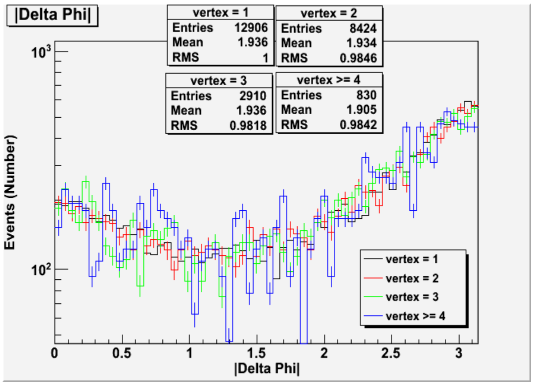

(c)

Fig. 22. |ΔØ| distributions at vertex = 1, 2, 3 and ≥ 4 for jet p_T cut 10 (a), 15 (b) and 30 GeV (c).

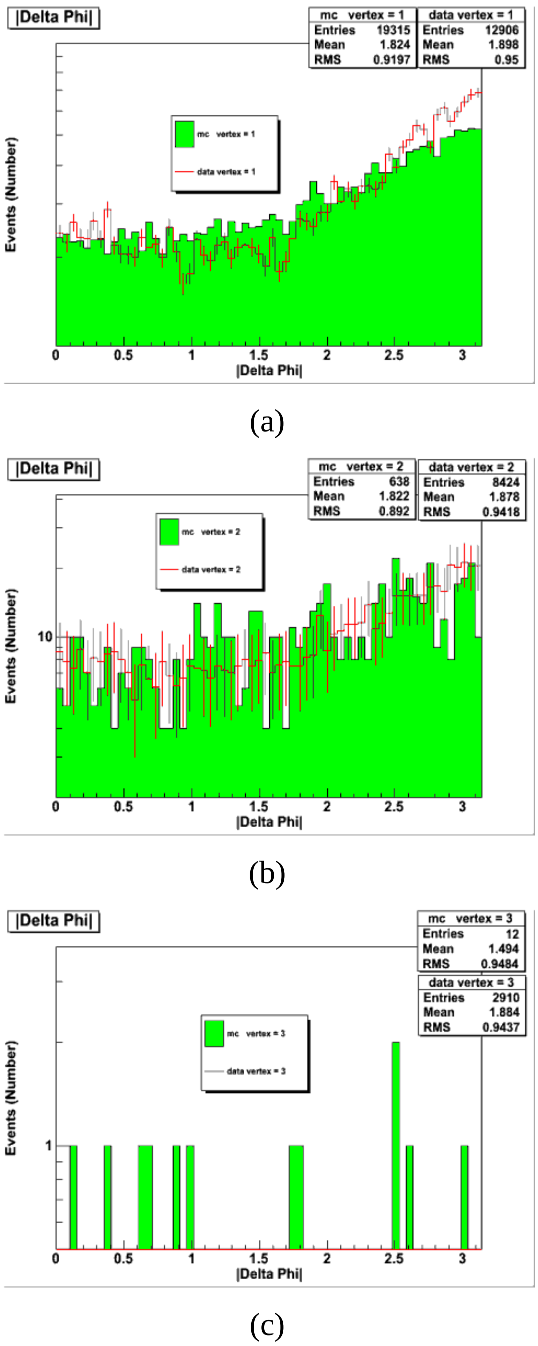

Fig. 23. Comparisons of |ΔØ| distributions between QCD_ p_T 15 and collision data with jet p_T cut 15 GeV at vertex = 1 (a), 2 (b) and 3 (c).

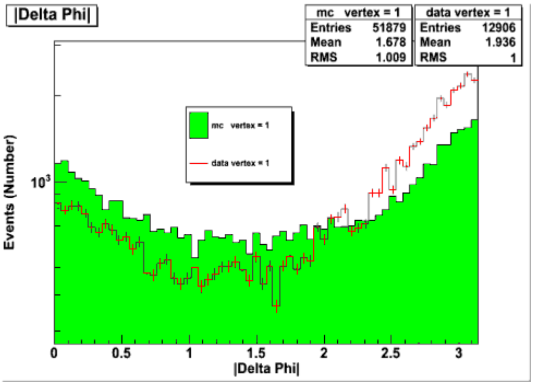

(a)

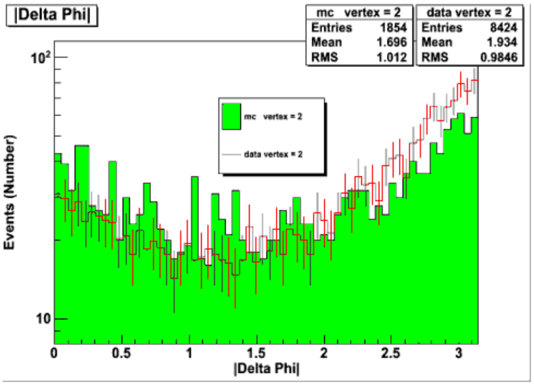

(b)

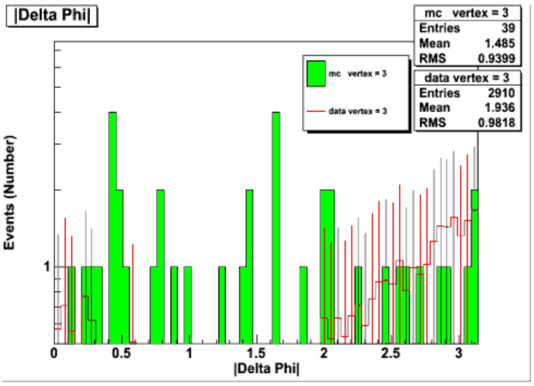

(c)

Fig. 24. Comparisons of |ΔØ| distributions between QCD_ p_T 30 and collision data with jet p_T cut 30 GeV at vertex = 1 (a), 2 (b) and 3 (c).

III. Conclusion

The event analysis codes was developed, which execute HT, MHT, MPT and |ΔØ | calculations with jet, photon, CaloJets and vertex processes to investigate pileup event effects with QCD_ p_T 15, QCD_ p_T 30 GeV MC and the LHC 7 TeV proton-proton collision data. The effect of pileup events was shown clearly in the magnitudes of track multiplicity, jet multiplicity and HT with jet p_T cut = 10 GeV. The mean of the track multiplicity at vertex = 2, 3 and ≥ 4 increased about 30, 57 and 83% respectively compared to the event of vertex one in the collision data with jet p_T cut 10 GeV. With the same conditions and comparisons, the pileup event effects appeared with the increment of about 10, 24 and 35% in jet multiplicity, 4, 10 and 16% in HT and 4, 9 and 18% in MHT for the mean value. The effects were most apparent in the track multiplicity. The correspondences between MC and collision data showed a good agreement with with jet p_T cut 30 GeV for the jet multiplicity, HT and MHT. The effect of pileup events was shown for MHT with the jet p_T cut 10 and 15 GeV with the increment of the MHT mean value at vertex = 2, 3 and ≥ 4 compared to vertex = 1 events. For the case of MPT distribution with jet p_T cut 30 GeV, the collision data was agreed well with the MC data. The |ΔØ| distributions of QCD_ p_T 30 GeV and collision data with jet p_T cut 30 GeV were well agreed showing expected enhancements near 0 and π.

IV. References

[1] Gordon Kane and Aaron Pierce, Perspectives on LHC physics (World Scientific 2008), Chap. 3.

[2] CMS Collaboration, CMS The Computing Project Technical Design Report, **CERN-LHCC-2005-023**, 3-71 (2005)

[3] CMS Collaboration, CMS Physics Technical Design Report Volume I: Detector Performance and Software **CERN/LHCC 2006-1**, 1-91 (2006).

[4] GEANT4 Collaboration, GEANT4: A Simulation Toolkit, NIM **A506**, 250 (2003).

[5] M. D'Alfonso, F. Garberson, S. A. Koay, S. Lowette, R. Rossin, M. Rydenfelt, J. Incandela, Missing Transverse Momentum of Tracks as an additional Handle for Missing Energy Based Searches, CMS **AN-2010/266**, 1-3 (2010).

[6] Riccardo Bellan, Mariarosaria D' Alfonso, Sue Ann Koay, Jia Fu Low, Steven Lowette, Roberto Rossin and Joseph Incandela, MPT Studies With First 7 TeV Collision Data, CMS **AN-2010-163**, 2 (2010).

[7] The CDF Collaboration, Search for the Standard Model Higgs boson in the missing energy plus jets sample, CDF **note 9483**, 1 (2008)

[8] The D0 Collaboration, A search for the standard model Higgs boson in the missing energy and a coplanar b-jet topology at $\sqrt{s}$ = 1.96 TeV, Fermi-lab **Pub-08/294-E**, 1 (2008)

[9] See https://twiki.cern.ch/twiki/bin/viewauth/CMS/SusyPatLayer1DefV9.

[10] T. Speer, K. Prokofiev, R. Fruhwirth, W. Waltenberger and P. Vanlaer, Vertex Fitting in the CMS Tracker, CMS NOTE **2006/032**, 4 (2006).

[11] Matteo Cacciari, Gavin P. Salam and Gregory Soyez, The anti-kt jet clustering algorithm, JHEP04 **063**, 2 (2008).

[12] See https://twiki.cern.ch/twiki/bin/view/CMS/WorkBookRunningGrid.

[13] See http://root.cern.ch/drupal.

[14] Jim Alexander, Freya Bleckman, Lawrence Gibbons, Aleko Khukhunaishvili and

Xin Shi, Missing transverse energy significance, algorithm description and implementation for various algorithm, CMS **AN-10-048**, 5 (2010).

요약

본 논문에서는 LHC 의 7 TeV 양성자-양성자 충돌실험 데이터의 중첩 event 와 비 중첩 event 의 track, jet, HT, MHT, MPT, $|\Delta\phi|$ 값들을 jet 의 transverse momentum cut 값과 primary vertex 수를 변화시키면서 비교 관찰하였다. 또한 같은 조건하에서 몬테카롤 시뮬레이션 데이터와 충돌실험 데이터 값들을 비교 분석하였다. 데이터분석에는 CMSSW_3_8_4, SusyPAT, Root 그리고 CRAB 이 사용되었다. 이벤트 데이터 분석코드는 C 언어로, 히스토그램 생성코드는 Python 언어로 작성되었다. 분석결과, 이벤트 중첩효과는 track 수에서 가장 잘 나타났다. 그리고, 몬테카롤 시뮬레이션 데이터와 충돌실험 데이터는 jet p_T 가 30 GeV 일 때 가장 잘 일치하였다. $|\Delta\phi|$ 분포 그래프는 QCD_ p_T 30 GeV 와 jet p_T cut 30 GeV 충돌실험 데이터들이 잘 일치함을 보여주었고, 예상했던 0 과 π 로의 편향성도 잘 보여주었다.